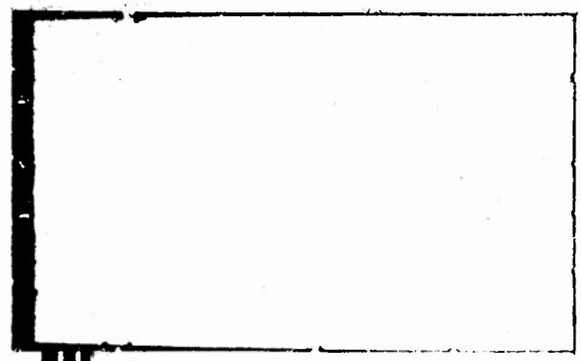

ELECTRICAL ENGINEERING RESEARCH LABORATORY
ENGINEERING EXPERIMENT STATION
UNIVERSITY OF ILLINOIS
URBANA, ILLINOIS

Copy No._____

PROGRESS REPORT ON GENERAL PROBLEMS OF BROADBAND AMPLIFICATION IN THE MICROWAVE FREQUENCY RANGE

N6-ori-71 Task XIX Report No. XIX-13

Date:

31 July 1951

Report for the Period:

31 March 1951

to

30 June 1951

Sponsored by:

United States Navy

Prepared by:

M.L. Babcock
L.R. Bloom
W.W. Cannon
T.N. Chin
D.F. Holshouser
R.J. Silverman
H.M. von Foerster

Approved by:

Heinz Von Foerster

H. M. von Foerster
Associate Professor

ELECTRON TUBE SECTION
ELECTRICAL ENGINEERING RESEARCH LABORATORY
ENGINEERING EXPERIMENT STATION
UNIVERSITY OF ILLINOIS
URBANA, ILLINOIS

TABLE OF CONTENTS

1. INTRODUCTION

This is the thirteenth quarterly progress report on the general problems of broadband amplification in the microwave frequency range. It is submitted in accordance with the terms of Contract No. N6-ori-71 Task XIX and covers the period 31 March 1951 to 30 June 1951.

2. THEORETICAL WORK

2.1 Stable and Quasistable Electron Clouds - H.M. Von Foerster

Evaluation of particular results presented in the two technical reports on Thermodynamics and Statistics of the Electron Gas (N6-ori-71 Task XIX TR 3-1 and 3-2) centered around the intriguing features of the spherical cathode (Report TR 3-1). It was thought that use could be made of the high electrostatic field on the inner-surface of the shell. Since this surface field upsets the boundary-conditions of the Child-Langmuir's space-charge law, an entirely different voltage-current characteristic should be expected (See Report TR 3-1, p. 24). To study this phenomenon with a feasible experimental setup, the case of the parallel-plane diode operating under retarding field-conditions is being considered again.

2.2 Parallel-Plane Diode - R.J. Silverman

To gain a better understanding of the parallel-plane diode, it is felt that the electron density, field and potential distributions need to be studied from a theoretical point of view in as much detail as possible. The Child-Langmuir law for the distributions of field and potential is in many cases not a good enough approximation to the actual situation. Around 1920 some work was done on the assumption of a Maxwellian distribution of the initial velocities of the electrons from the cathode. While the basic equations derived from this assumption seem correct, this work is incomplete in many respects.

1. Only the case where a potential minimum is attained within the cathode is considered.
2. Only approximate solutions were attained.
3. The form of the initial equations are rather unwieldy and do not lend themselves readily to physical interpretation.
4. Numerical and graphical results are few and these are difficult to use.

The analysis of this problem, which was started at the end of June, will be conducted with the above four points in mind.

2.3 Electron Flow in a Parallel-Plane Diode - T.N. Chin

The aim of this study is to attempt to quantitatively determine tube characteristics that are not directly measurable. The general lines along which it is proceeding have been outlined in the last quarterly report.

Before making further theoretical studies along this line, it is worth while to verify experimentally some of the derived relations. In this treatment a microscopic quantity -- electron temperature -- is defined to describe the velocity spreading of a group of electrons. R. Champeix[1] reported some work on the comparison between the electronic temperature and the thermodynamic temperature of oxide cathodes. In his work the parallel-plane diode was used and electronic temperatures were evaluated from the retarding field measurements of the anode.

1. R. Champeix. Comparaison entre la température électronique et la température thermodynamique des cathodes à Oxydes," Compt. Rend. Acad. Sci., Paris, 1950, Vol. 64, P. 230.

With the same purpose in mind, experiments were performed during the last period. The set-up used a 0.001-in. probe between the cathode and the anode. The electron temperatures were evaluated from the probe measurements. Results indicated that the electron temperature is very close to the cathode temperature.

In a gas discharge tube a sheath around the probe is visible. It is generally assumed, or at least hoped, that the probe does not seriously disturb the discharge beyond the limits of the sheath. However, this assumption does not seem to be valid in the vacuum tube case. From the data obtained, one may be inclined to think that in the relatively negative potential of the probe characteristics the current may arise from the electron group close to the cathode, and in the relatively small potential of the probe characteristics the current may arise from the electron group close to the probe. Unfortunately it is not possible to draw a conclusion from this experiment.

3. EXPERIMENTAL WORK

3.1 Stable Spherical Electron Cloud - D.F. Holhouser

The experimental phase of the study of the thermodynamic properties of a stable electron cloud, which has previously been carried out under another contract, has been transferred to the subject contract and is reported herein. The objective of the experiments is to obtain data to compare with the analysis described in Technical Report No. 3-1. In that report the properties of an electron gas, produced by thermionic emission from the inner surface of a closed spherical shell, are analyzed.

To test these results experimentally, a spherical cathode with 1 cm radius was designed. A cross section of the device is shown in Fig. 1 and a photograph in Fig. 2. The cathode is heated by an external concentric sphere. The inner surface of the cathode is coated with an oxide emitting material. Information on the electron gas is obtained by collecting the electrons emerging from a small (1 mm diameter) aperture in the cathode.

From the expressions for electron density and current through the aperture given in the above mentioned report.

$$n_o = \frac{2\pi m K^2 T^2}{h^3} \sqrt{2m/e(U_o + \phi_o)} \; \epsilon^{-\frac{e\phi_o}{KT}} \tag{1}$$

and

$$j = n_o e \left(\frac{3KT}{m}\right)^{1/2} \tag{2}$$

the current through the hole is found to be

$$j = \frac{3K}{8e(U_o + \phi_o)} A_o T^{5/2} \epsilon^{-\frac{e\phi_o}{KT}} \tag{3}$$

$$= A_1 T^{5/2} \epsilon^{-\frac{e\phi_o}{KT}}$$

Measurements of saturated current for several temperatures were made and the values of work function, ϕ_o, and A_1 were found to be

$$\phi_o = 2.3 \text{ volts}$$

$$A_1 = 5 \times 10^5 \text{ amp} \cdot \text{m}^{-2} \cdot {}^{\circ}\text{K}^{-5/2}.$$

The work function is considerably higher than that of a well-activated oxide-cathode, but this may be due to the geometry which prevents application of an electrostatic field during activation.

According to the analysis a field exists at the emitting surface which would give electrons an initial acceleration through the aperture and thus not meet the conditions of the Childs-Langmuir space-charge-limited emission. As a consequence one would expect saturation currents

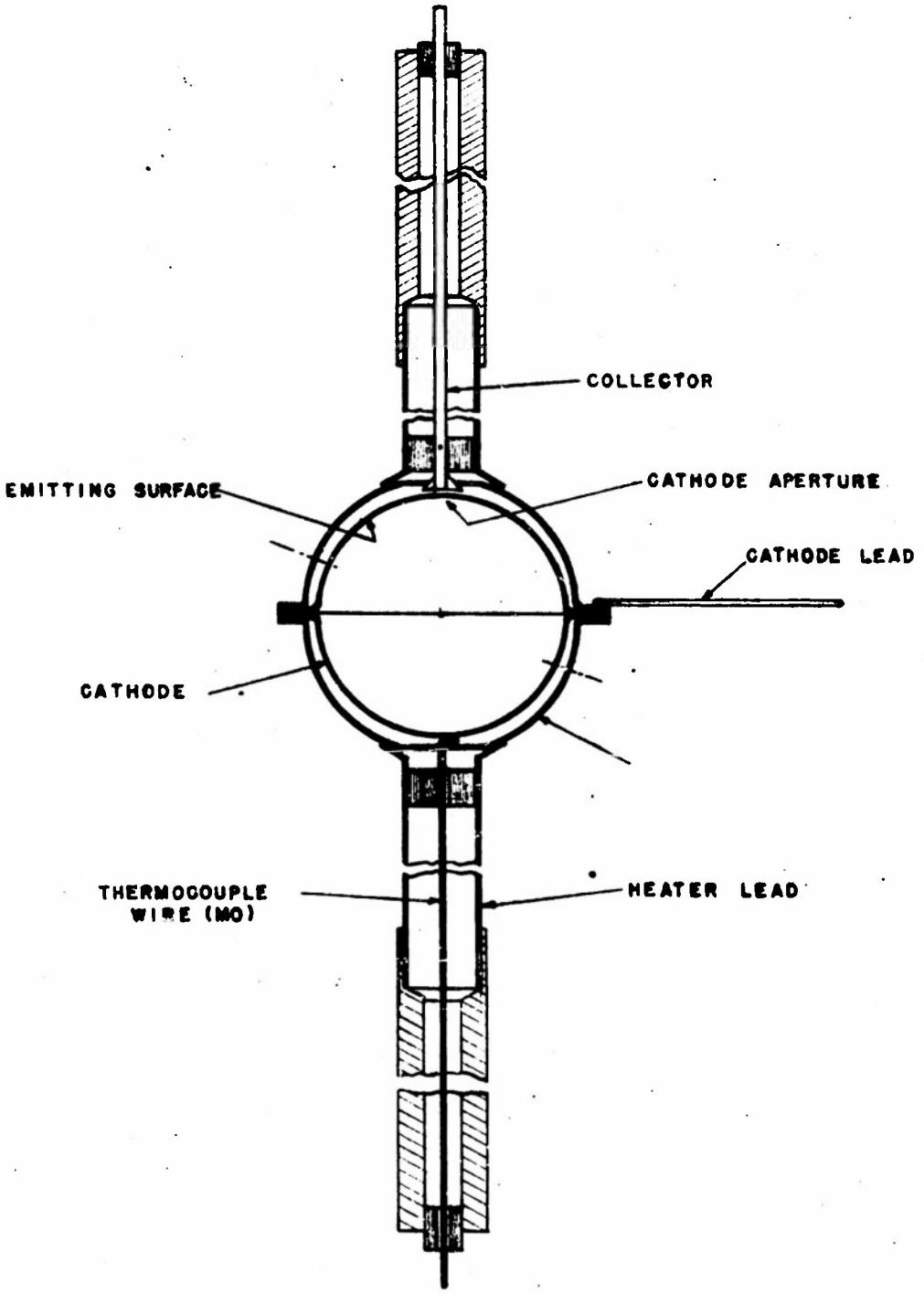

Figure 1
Spherical Cathode Assembly

Department of Electrical Engineering — University of Illinois

DWG NO. 1768-1

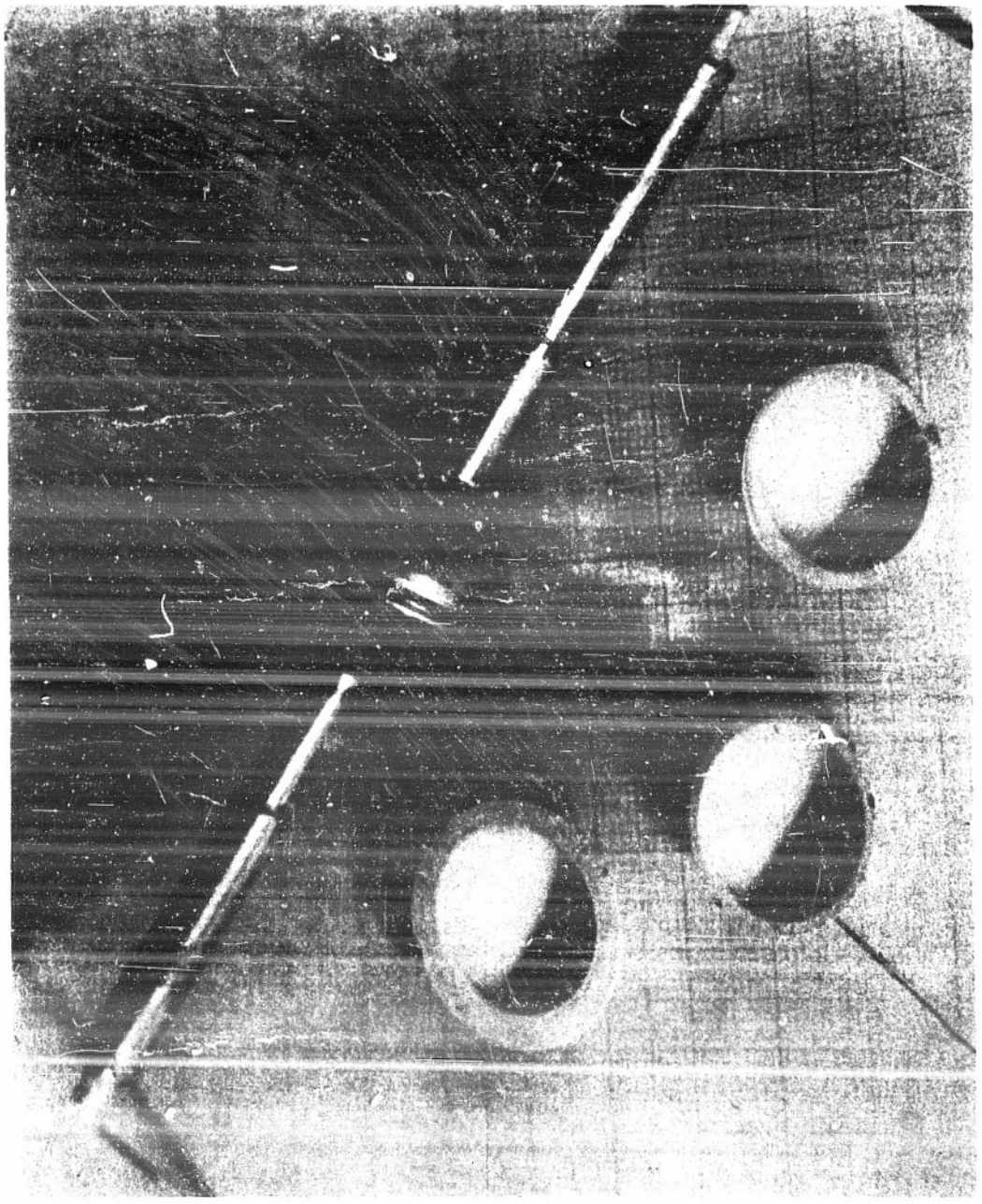

Figure 2
Photograph of Spherical Cathode Assembly

to be collected even for very small positive collector potentials. Figure 3 shows the measured aperture current characteristic as compared to a convential diode of the same dimensions. Indeed, it appears that a field exists at the aperture which gives saturation at low applied potentials. Unfortunately, this data is inconclusive since for applied negative potentials a positive ion current was observed.

It can be shown that

$$\frac{\rho_o^-}{\rho_o^+} = \frac{i_s^-}{i_s^+} \left(\frac{m^-}{m^+}\right)^{1/2} \tag{4}$$

where ρ_o is charge density at the aperture, i_s is saturation current, m is the mass of charged particle, and the signs indicate electrons or positive ions. Since $m^-/m^+ \cong 10^{-4}$ and $i_s^-/i_s^+ \cong 10^2$ from the measured values, then $\rho_o^-/\rho_o^+ \cong 1$. This indicates space-charge compensation at the aperture, and as a consequence the initial field could be the result of applied potential rather than the electron distribution within the sphere. It should be noted that this ionization is produced by electrons having only thermal velocities.

3.2 Traveling-Wave Tube - M.L. Babcock

The conductivity tests of the Alsimag 222 ceramic showed that it will be satisfactory as a replacement for the Grade A Lava in the Heil gun. However, it has not been incorporated in the gun design as yet.

The Heil gun has not been redesigned mechanically and will be tested during the next quarter for use in the magnetic-washer beam guide. It is now becoming apparent that if the accelerating electrode current of the Heil gun cannot be decreased then the gun will have to be abandoned. The operation of this gun is very dependent upon the pressure under which it is operated since higher pressures apparently disturb the cathode space-charge region to the extent that the electron trajectories are not correct for a parallel beam. Thus it is possible that the Heil gun will not be a good experimental gun for use in the proposed magnetic-washer beam guide.

With the above thought in mind, some time has been spent in preliminary tests of the Philips L-cathode. These have shown promise. A tremendous amount of trouble has been caused by poor heaters in the L-cathode. None of the heaters used thus far have remained intact long enough to activate and age a cathode. However by rapid replacement of heaters, one L-cathode has been activated and aged properly and operated for a short length of time. This test was a simple diode test. An emission current having a density of 4.5 amp/sq cm of cathode surface was obtained in this test with cathode temperature of 1300°C. At this emission density, temperature limitation of the emission was beginning to appear. At this point the heater burned out and when it was replaced, attempts to reactivate the cathode failed. However, since the L-cathode appears to be promising, further tests are to be conducted.

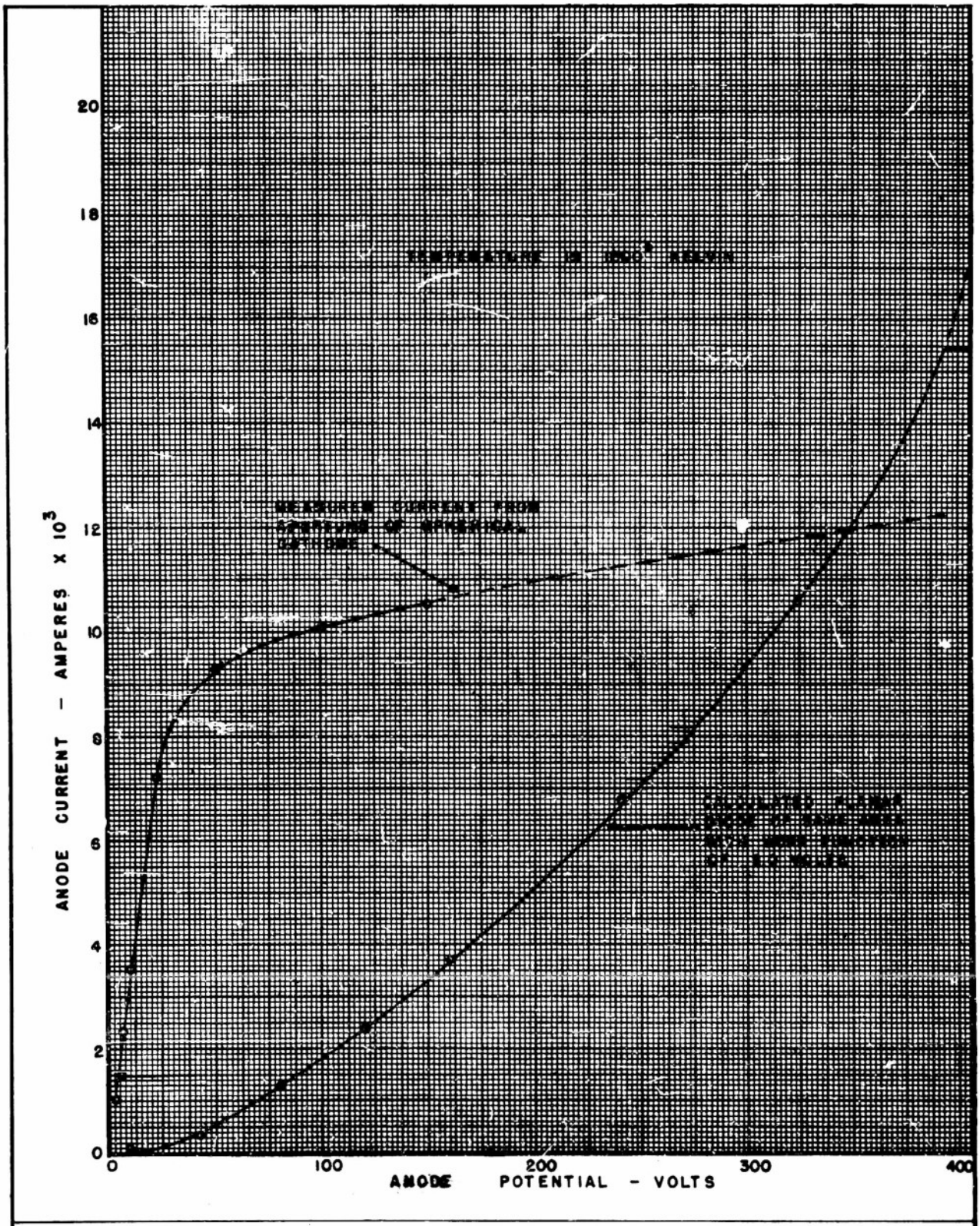

FIGURE 3

COMPARISON OF SPHERICAL-CATHODE APERTURE CHARACTERISTIC AND CALCULATED PLANAR DIODE CHARACTERISTIC

As reported in the last report, a plotting tank model of the magnetic-washer beam guide was set up and the resulting fields studied. Considerable time was spent in trying to analyze the resulting field plots and also trying to plot electron paths. The results were very disappointing. No ready method of plotting paths analytically or graphically was available. Also it was decided that the field plots obtained with the electrolytic tank were not faithful enough representations of the true fields since any small error made in plotting would be multiplied over the length of the magnetic beam guide when this plot was used to determine the electron path. Therefore this method of analysis has been abandoned.

$$\theta = \frac{n\pi \times 10^3}{\sqrt{V_o}} \left(\frac{K}{1+K}\right) \quad (5)$$

where $K = \frac{\Delta v}{v_o}$ is the velocity modulation

$n = \frac{S}{\lambda}$

S = spacing between the systems

$\lambda = \frac{c}{f}$ is the free-space wavelength of the deflecting signals

θ = Phase shift

V_o = Beam voltage

However, the upper value of beam voltage is limited by the deflection sensitivity required.

This smearing caused by velocity modulation may be used to advantage, if one is willing to accept a nonlinear phase sweep. If the first deflection system produces deflection in the y-direction, then this direction can be taken as the reference point for phase and the picture on the screen will always represent phase according to $y = A \sin \phi$, independently of the distance to the second system. If we are willing to accept this representation of phase in the beam we may accent the smearing in the x-direction by increasing the separation of the two deflection systems. Then the x-deflection can be interpreted as a measure of the degree of velocity modulation.

Let the circle

$$\begin{aligned} x &= A \sin \phi \\ y &= A \cos \phi \end{aligned} \quad (6)$$

be the reference. Then any new trace caused by velocity variation may be represented by

$$\begin{aligned} x &= A \sin (\phi + \theta) \\ y &= A \cos \phi \end{aligned} \quad (7)$$

where ϕ is the phase in the beam with reference to the y-deflection system, and θ is a function of the velocity change and spacing given by Eq. 5.

Letting Δx be the x-displacement from the circle,

$$\begin{aligned} \Delta x &= A [\sin (\phi + \theta) - \sin \phi] \\ &= A [(\cos \theta - 1) \sin \phi + \sin \theta \cos \phi \end{aligned} \quad (8)$$

where again θ is given by Eq. 5.

The velocity sensitivity of such a device may be widely varied by changing the spacing between the deflection systems or by changing the beam voltage. However, the phase-velocity picture obtained on a screen by this method will not be single-valued in phase and velocity. Some portions of the picture may represent multiple values of velocity or multiple values of phase or both, but the sensitivity may be adjusted so that a portion of the picture representing a $\Delta\phi$ (or Δy) will be single-valued in both phase and velocity. In Fig. 5 region (1) is single-valued in phase and velocity, region (2) is double-valued in phase and single-valued in velocity, while region (3) is double-valued in both velocity and phase.

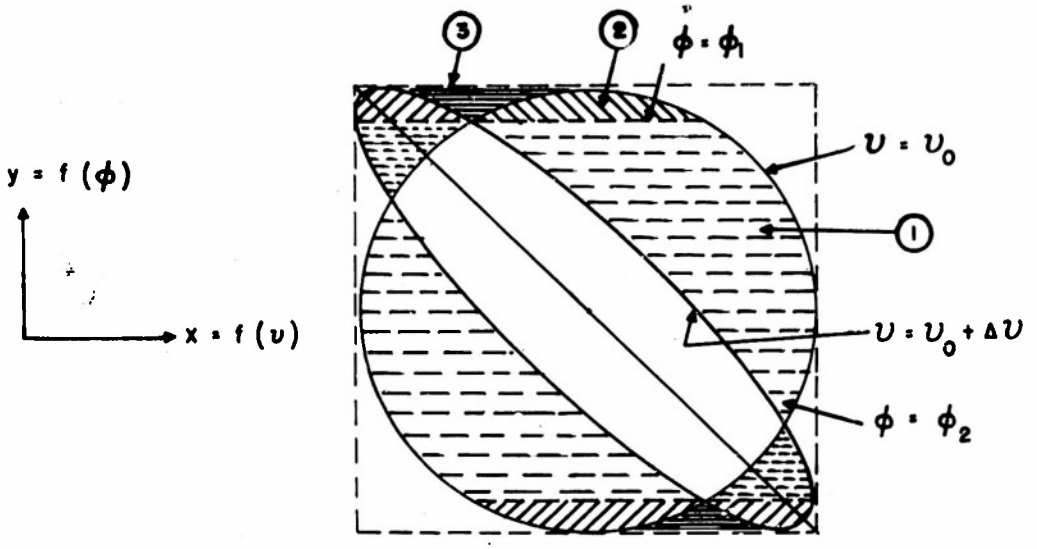

FIGURE 5

The beam may be sampled at the input by the beam chopped in such a manner that only the single-valued portion of the picture is obtained and the time (or phase) of sampling may be adjusted so that every phase interval in the beam may be examined in sequence. Or without resorting to sampling, the time of entry of the beam into the first deflection system (or reference phase) may be varied such that all phases of the beam may be made to pass in sequence through region (1) of the picture. Phase as used here represents time-phase of modulation in the electron beam with the first deflection system as the reference position.

This circular sweep, because of the high angular velocity which may be obtained, offers many interesting possibilities for future investigation. We have, for several years, been wanting such a sweep for investigating the space-charge distribution in a magnetron. With a sweep having an angular velocity of 3000 mc/sec passing axially through an oscillating magnetron, one should obtain a picture of the angular configuration of space charge. This particular problem cannot be attacked very readily with a dc beam without a synchronous sweep. It is also suggested that such a rapid sweep could be used to measure a function which occurs in extremely short time intervals.

4.2 Velocity Spectrograph

An attempt is being made to design a velocity-sensitive device which will operate in conjunction with the circular sweep. This device should cause a deviation in the radius of the phase circle as an indication of velocity deviation from a mean value. The first structure investigated had a shape obtained by revolving two concentric circle segments about an axis lying outside the circles, as shown in Fig. 6. The surfaces thus formed are segments of concentric toroids, but LaPlace's equation is not separable in such coordinates, making the solution for the fields quite a difficult task. Therefore other methods are being investigated.

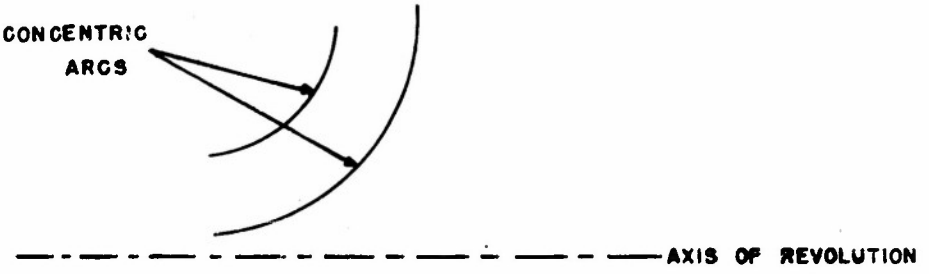

FIGURE 6

4.3 Beam Chopper

The beam chopper described in the last report, which consists of one parallel-wire deflection system sweeping a beam past a narrow aperture, was investigated further. It was found that with a beam voltage of 900 v, a sweep frequency of 3000 mc, and a sweep amplitude of ten times the aperture width, the space duration of the bunches so formed would be about 1/3 the aperture width. Or for an aperture 1 mm wide the bunch would be 0.3 mm long in the direction of travel. However, in a direction slightly askew from the direction of travel, the bunch thickness is only 1/6 the beam diameter.

Bunches of such short duration may find many uses. However, bunches formed in this manner cannot have a density greater than the original beam density without some further maneuvering.

4.4 Construction of the Beam Analyzer

An analyzer is being constructed with a steel housing of square cross section. It is being built of modular construction so that units may be added or rearranged for different schemes of operation.

5. CONCENTRIC LINE POWER METER

L.R. Bloom, W.W. Cannon

In Progress Report No. XIX - 8 of May 1950 was suggested a system for producing a velocity-modulated test beam for checking the characteristics of the "beam analyzer." The method was that of firing a beam diametrically through a concentric line which is transmitting power. Modulation of the electron beam would then be due to accelerating and decelerating forces acting on the beam as it passes across the cylindrical gaps of the line. If a known amount of power flows down the line then the extent of the velocity-modulation on the beam is determined.

A somewhat different purpose has been suggested and since applied to such structures. Since the peak energy gained by an electron beam in passing through a concentric line is measurable, and since the gain in energy is related to the r-f voltage in the concentric line, this makes a promising method for measurement of r-f power.

The following is a description of a "concentric line power meter" together with a summary of analytic and experimental results.

5.1 Principle of Operation

In Fig. 7 is shown a cross-section of a concentric line through which is bored a small hole passing through the center of the inner conductor. A cathode ray-type of gun fires an electron beam across the concentric line and the electrons are collected externally by means of a collector electrode. An electrostatic voltmeter of very high impedance is connected between cathode and collector. With no r-f on the line the collector will charge up to cathode potential and the net voltage on the electrostatic voltmeter will be zero. With an r-f field on the concentric line and the beam voltage properly chosen some electrons will gain energy in transit across the gaps and will exhibit a voltage on the collector which is proportional to the fields in the line.

The analysis of this system assumes the fields across the concentric line to be constant with the radius r. It is also assumed that there is no distortion of the fields due to the holes in the line. The analysis is given in the attached appendix which relates the peak voltage gained by the electrons to the r-f power in the line for a given line geometry, beam voltage and frequency of r-f signal.

The formula relating these quantities is as follows:

$$\frac{\Delta V}{|V_\sim|} = \frac{\sin\frac{\phi_1}{2}}{\frac{\phi_1}{2}} \sin\left(\frac{\phi_1 + \phi_2}{2}\right) \qquad (9)$$

where ΔV is the peak voltage on the collector electrode, $V_\sim$ is the voltage across the gap, ϕ_1 and ϕ_2 are the transit angles across the 1st gap and the drift region, respectively.

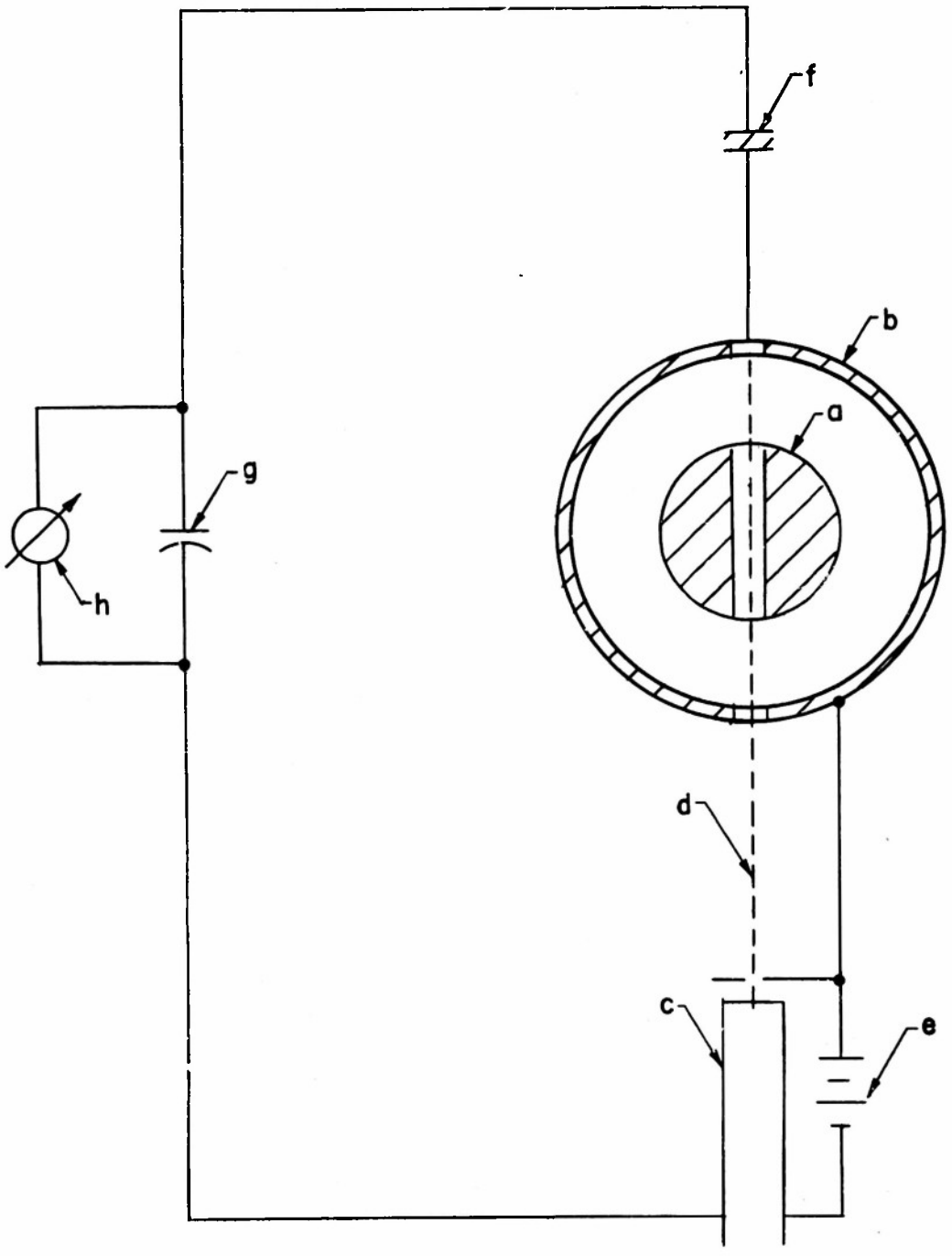

FIGURE 7 SCHEMATIC OF RF PEAK POWER METER

The transit angle ϕ_1 is related to the beam voltage and the geometry by the expression

$$\phi_1 = \frac{2\pi\tau}{T} = \frac{2\pi S_1}{v_o T}$$

where τ is the transit time $\frac{S_1}{v_o}$, S_1 is the gap spacing, v_o the velocity of the beam and T is the period of oscillation of the r-f field, $\frac{1}{f}$.

$|V_\sim|$ is determined from the input power and the characteristic impedance of the line by the well-known relation $V_\sim = \sqrt{2P_Z}$.

For a given geometry of line and constant r-f power input the Eq. 9 may be written as

$$F = \frac{\sin \frac{\phi_1}{2}}{\frac{\phi_1}{2}} \sin \left(\frac{\phi_1 + \phi_2}{2}\right) \tag{10}$$

or further reduced to the expression

$$F = \frac{\sin \frac{A}{v}}{\frac{A}{v}} \sin \frac{B}{v} \tag{11}$$

where v is the velocity at a given beam voltage. If the function F is differentiated with respect to v and set equal to zero, the conditions for maximum sensitivity may be readily obtained as given by the expression

$$\frac{\frac{\phi}{2}}{\tan \frac{\phi}{2}} + \frac{\frac{\phi_1}{2}}{\tan \frac{\phi_1}{2}} = 1 \tag{12}$$

where

$$\phi = \phi_1 + \phi_2$$

A concentric line power meter was designed and built as shown in the drawing, Fig. 8a and photograph Fig. 8b.

The concentric line was designed with the following geometry:

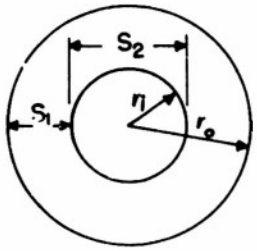

$2R_o = 0.675$ cm
$2R_i = 0.320$ cm
$S_1 = 0.180$ cm
$S_2 = 0.320$
$Z_o = 45\ \Omega$

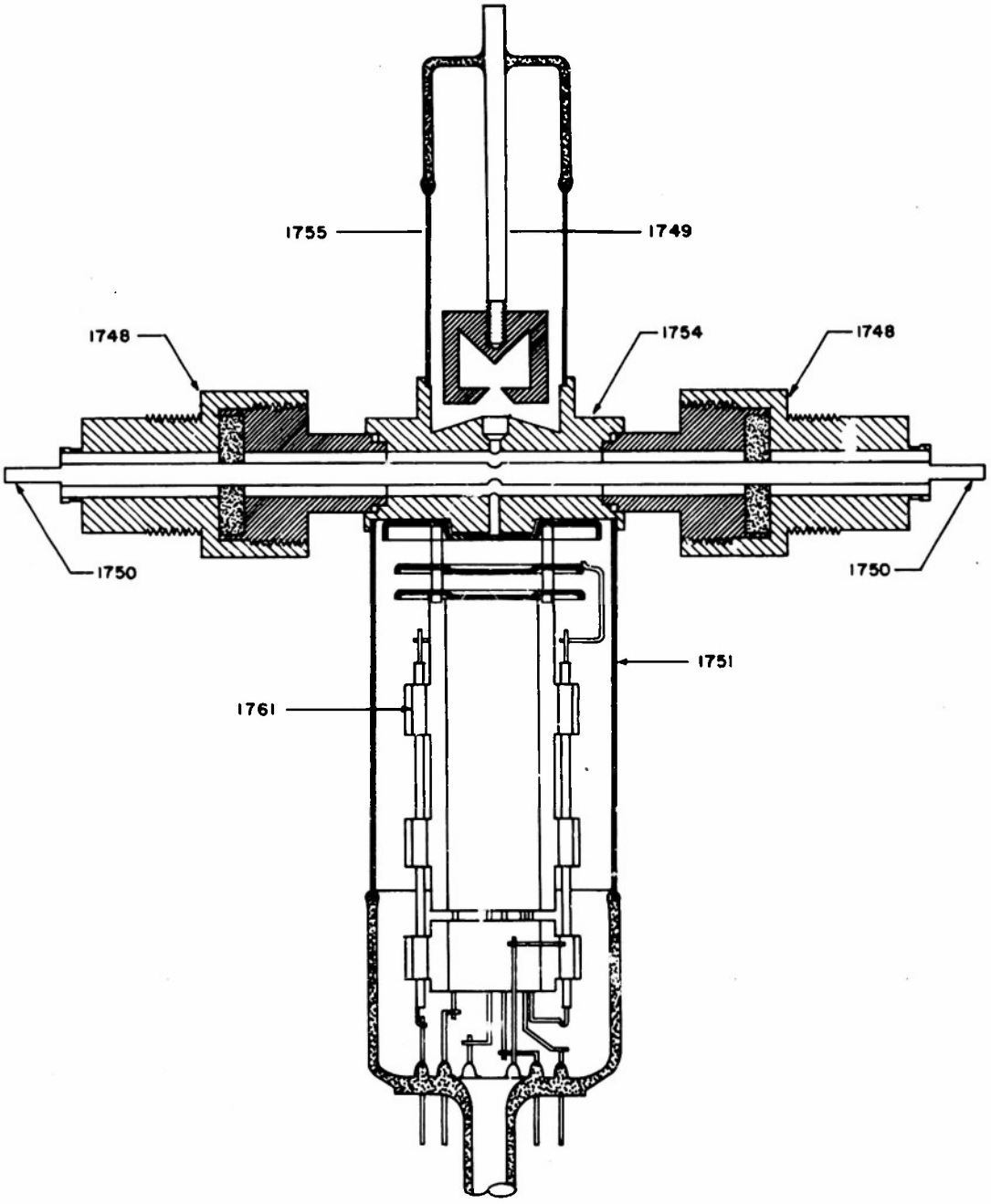

FIGURE 8A
A COAXIAL POWER METER

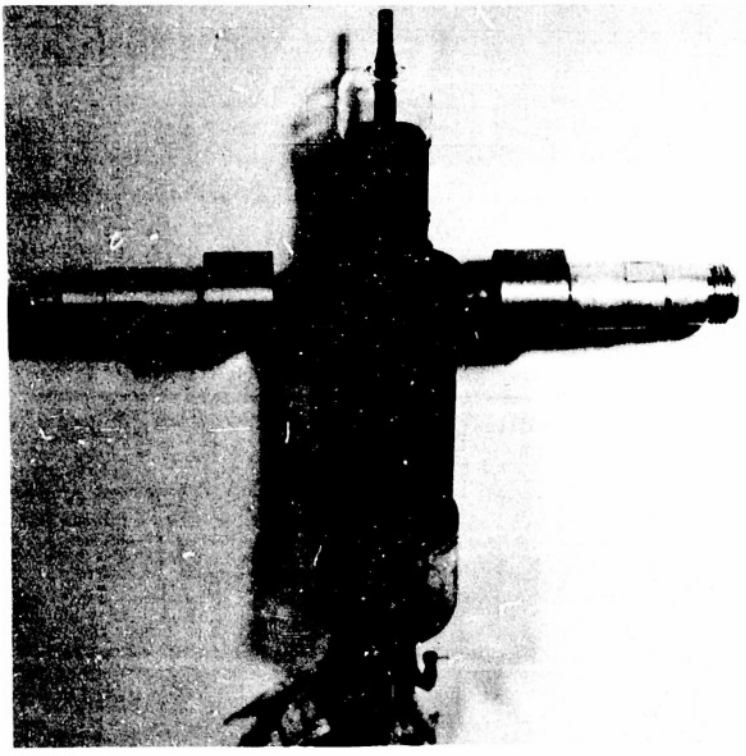

FIGURE 8B
CONCENTRIC LINE R-F POWER METER

With these values given and assuming fixed power input, a theoretical plot was made of the function of Eq. (9). This curve is given in Fig. 9. Zero values for sensitivity are obtained by specifying the beam voltages for which

$$\sin \frac{\phi_1}{2} = 0 \quad \text{and} \quad \sin \frac{\phi_1 + \phi_2}{2} = 0$$

These values occur when

$$\frac{\phi_1}{2} = n\pi; \qquad \frac{\phi_1 + \phi_2}{2} = n\pi \qquad n = 1, 2, 3, - - - -$$

Maximum values obtain directly from the relation Eq. (12).

5.2 Experimental Results

The experimental procedure was to design the concentric line power meter so as to provide a section of the line with a minimum discontinuity due to coupling links. Essentially the section of the concentric line should be non-resonant, since standing waves would increase the fields through which the electrons would pass and thus introduce an additional factor in the interpretation of the measured values.

Measurements were made to check the theoretical curve of Fig. 9, by plotting the readings on the electrostatic voltmeter as a function of beam voltage fixing power and frequency. The results of these measurements are plotted on the same curve as a series of small circles.

Measurements were also made of the electrostatic voltmeter readings as a function of the power in the line for a fixed beam voltage. These results are plotted in Fig. 10.

An examination of the results show that with a second-order finite-gap approximation of Klystron theory a powerful tool is made available for prediction of high frequency effects. This is shown by the rather good agreement between the theoretical curve based on finite-gap theory and the experimental results.

Some of the advantages of such a system are

1. Essentially no power is removed from the system
2. Minimum distortion of the r-f power flow down the line
3. Extreme stability as a function of beam voltage as evidenced by the flat plateau of the lst maximum
4. Reasonable insensitivity to the geometrical proportions of the system.

The advantage stated in (4) above may be readily seen from the curve of Fig. 11. The values of f(x) plotted on the graph indicate the small change in the height of the lst maximum as a function of the ratio of the gap lengths S_2/S_1.

The curve is obtained by simultaneous solution of the two transcendental functions

$$f(x) = \frac{\sin x}{x} \sin y$$

and

$$\frac{x}{\tan x} + \frac{y}{\tan y} = 1$$

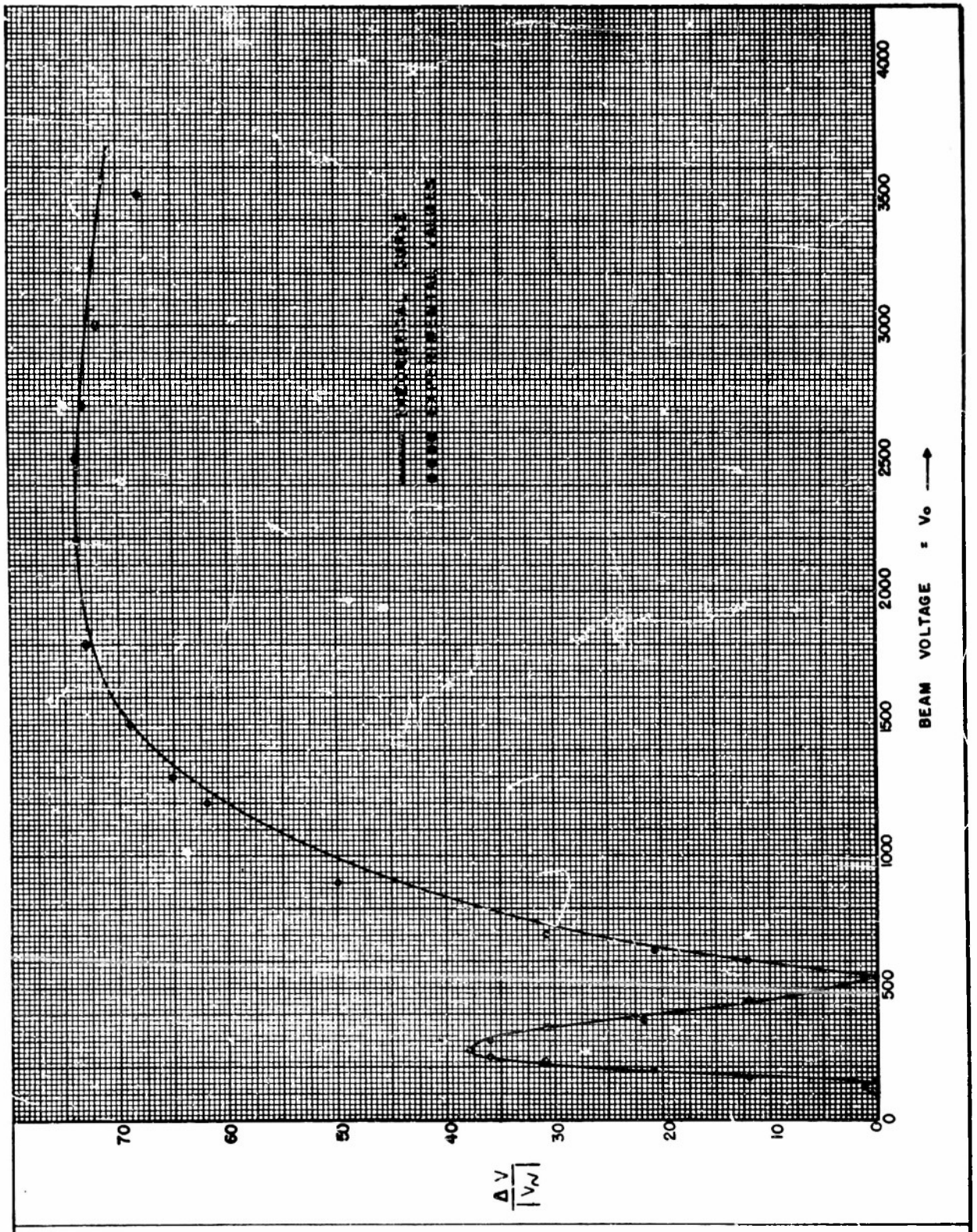

FIGURE 9

RATIO OF COLLECTOR VOLTAGE TO GAP VOLTAGE FOR R-F POWER METER

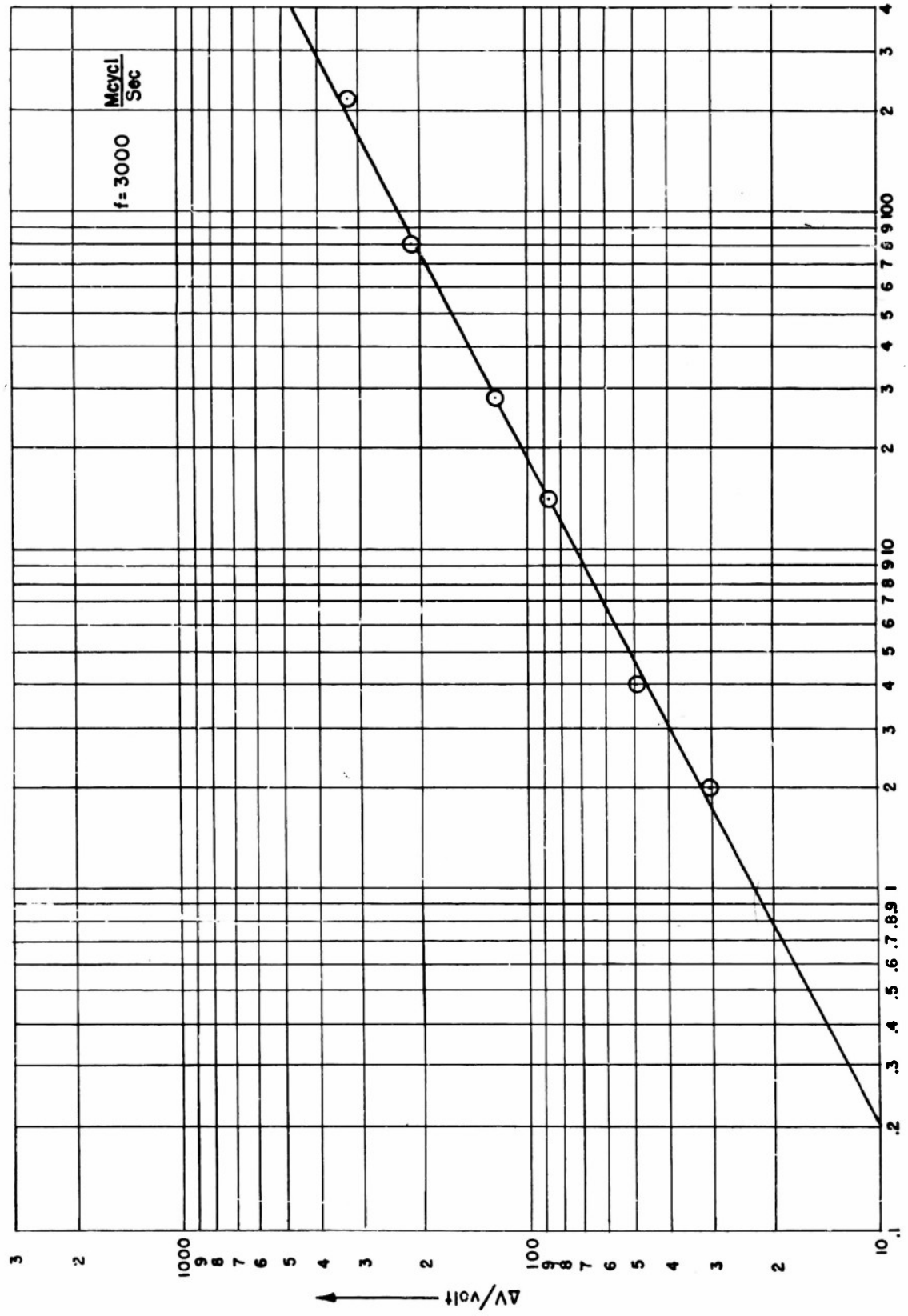

FIGURE 10 CONDENSER VOLTAGE VS. SQUARE ROOT OF SIGNAL POWER

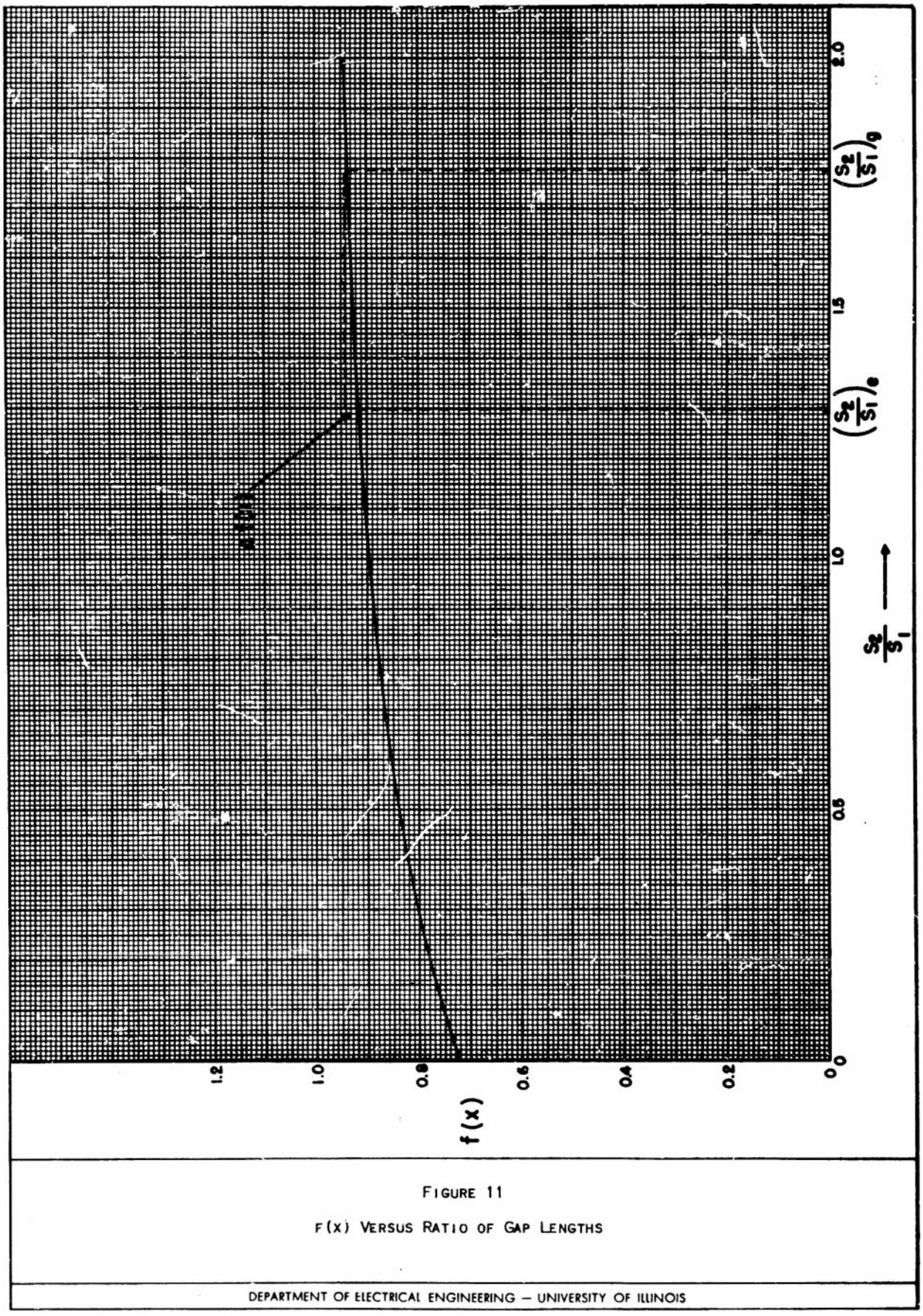

FIGURE 11

F(X) VERSUS RATIO OF GAP LENGTHS

DEPARTMENT OF ELECTRICAL ENGINEERING — UNIVERSITY OF ILLINOIS

where $\frac{S_1}{S_2} = \frac{y}{x} - 1$

The values $(\frac{S_2}{S_1})_g$ and $(\frac{S_2}{S_1})_e$ are the ratios of the real gap spacing and the effective gap spacing.

This discrepancy between the two ratios can be understood if one visualizes that in the simple theory no account was taken of the distortion of the fields in the gap region due to the holes. The expansion of the fields into the holes as shown in Fig. 12 make it clear that the

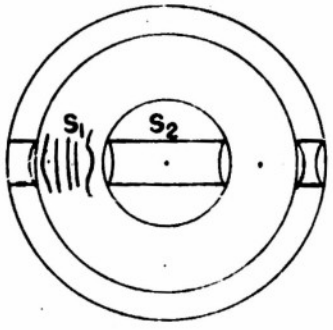

FIGURE 12

inner gap S_2 becomes in effect smaller and the other gap S_1 larger so that the effective ratio of $(\frac{S_2}{S_1})_e$ becomes smaller.

6. PLANS FOR THE NEXT INTERVAL

6.1 Stable Spherical Electron Cloud

An aperture diode with planar rather than spherical surfaces will be constructed. This will permit more efficient pumping and activation.

6.2 Parallel-Plane Diode

In the next period, another experimental set-up different from that described in Section 3.2 will be designed. A small hole is to be provided in the anode and the collectors will be outside the cathode-anode space. The intention is to investigate the electron group close to the anode with the hope that the disturbance arising from the collectors will be very small.

6.3 Electron Beam Analyzer

It is planned to investigate other types of velocity discriminating structures and have one built, if a satisfactory one is found. The demountable model shall be completed and tested for consistency with the previous experiments.

6.4 Concentric Line Power Meter

1. Measurements will be made with the concentric line power meter to determine effects of standing waves inside the line.
2. Reliability of readings as function of frequency will be determined.
3. A technical report will be prepared giving in detail the results of this investigation.

6.5 Traveling-Wave Tube

The immediate plans for the next interval are (1) the experimental testing of the magnetic-washer beam guide using the redesigned Heil gun and (2) further tests of the L-cathode. If these latter tests prove satisfactory then the L-cathode will be used as the emission surface of a Pierce-type structure for the production of a high intensity electron beam.

4. ELECTRON BEAM ANALYZER

W. W. Cannon, L. R. Bloom

4.1 Phase Writer

The circular-phase sweep mentioned in the last report has been investigated further. In order to have a perfect circle the effective phase difference in signals between the two deflection systems as seen by an electron passing through them must be 90°. This phase difference is, of course, dependent upon the velocity of the electron. If we have a beam of uniform velocity v_o then the phase difference in the applied signals may be adjusted so that the Lissajous figure on a screen will be a circle. Then a change in velocity will cause the figure to change from circle to ellipse to straight line and back again with the direction of trace being reversed when the figure passes through the straight line stage.

If we now pass a beam through the two consecutive perpendicular deflection systems upon which an r-f signal is impressed so that a uniform beam velocity v_o produces a circle on the screen and then velocity modulate the beam so that its velocity limits are v_o and $v_o + \Delta v$, a figure will be obtained on the screen having its boundary smeared between a circle and an ellipse as shown in Fig. 4. This velocity smearing of the

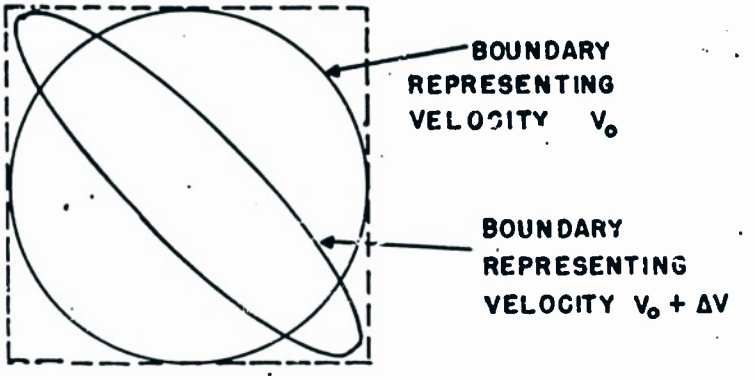

FIGURE 4

Lissajous circle is a distinct detriment if it is desired to display the phase of a velocity modulated beam as a purely polar picture.

Assuming that in the phase circle it is desirable to obtain a phase resolution of 10° and we cannot place our deflection systems closer than 5 mm, we can calculate the maximum velocity modulation permissible without destroying the phase resolution. For a beam voltage of 900 v the maximum permissible velocity modulation would be 3.5% at 3000 mc. If, on the other hand, a velocity modulation of 33⅓% and a beam voltage of 900 v are specified, then the deflection systems must be spaced 0.7 mm in order to maintain a phase resolution of 10°. This small spacing is difficult to achieve. Of course higher voltages permit greater spacings. These quantities are related by the formula: